

# A NEW CONSERVATION LAW DESCRIPTION OF AN ELECTROMAGNETIC ACOUSTIC TRANSDUCER IN THE TIME DOMAIN

R. Ludwig and X.-W. Dai

Department of Electrical Engineering  
Worcester Polytechnic Institute  
Worcester, MA 01609

R. Palanisamy

Timken Research  
Canton, OH 44706

## INTRODUCTION

This paper presents a unified theoretical formulation describing the electrodynamic transduction process governing the transmitter behavior of an Electromagnetic Acoustic Transducer (EMAT) in the time domain. This new approach establishes separate electrical, mechanical and material formulations, so-called subsystems, based on momentum conservation forms of Maxwell's field equations in the quasi-static limit and Cauchy's law of motion. Thus, instead of accounting for the electromagnetic acoustic material interaction by direct linkage of mechanical stress tensor and magnetic flux density via constitutive relations [1], the coupling of the field tensors is achieved by relying on a material subsystem. This subsystem, which takes into account the specimen, interfaces between the electrical and mechanical subsystems in a self-consistent way. As a result, the complete set of governing equations and associated boundary conditions can be derived from first principles.

The numerical implementation of this model permits the study of transient acoustic radiation patterns as a function of EMAT transmitter parameters. As an example, the influence of variable versus fixed transmitter coil lift-off and associated meander wire spacing is examined in terms of various Lorentz force distributions and their associated bulk and surface wave radiation patterns.

## THEORETICAL STRATEGY

The general theoretical approach of formulating the momentum conservation law description requires the establishment of three subsystems. The first or electric subsystem is described by

$$\nabla \cdot \mathbf{T}_e + \frac{\partial \mathbf{G}_e}{\partial t} = \mathbf{f}_e \quad (1)$$

where the Maxwell stress tensor in terms of the magnetic field  $\mathbf{H}$  and the permeability  $\mu_0$  is given by

$$\mathbf{T}_e = \frac{1}{2} \mu_0 |\mathbf{H}|^2 \mathbf{I} - \mu_0 \mathbf{H} \mathbf{H} \quad (2)$$

$\mathbf{I}$  is the identity matrix. Since we are concerned with only low-frequency electromagnetic fields,  $\mathbf{G}_e = \mathbf{0}$ . The force density is specified in terms of magnetization vector  $\mathbf{M}$  and induced current density  $\mathbf{J}_e$  in the specimen as

$$\mathbf{f}_e = -\mathbf{J}_e \times \mu_0 \mathbf{H} - \mathbf{H} (\nabla \cdot (\mu_0 \mathbf{M})) \quad (3)$$

The second or mechanical subsystem is formulated in a similar form as

$$\nabla \cdot \mathbf{T}_k + \frac{\partial \mathbf{G}_k}{\partial t} = \mathbf{f}_k \quad (4)$$

with the kinetic stress tensor expressed in terms of material tensor  $\mathbf{c}$  and particle displacement vector  $\mathbf{u}$  as

$$\mathbf{T}_k = -\mathbf{c} : \nabla \mathbf{u} \quad (5)$$

The moment of momentum is given by

$$\mathbf{G}_k = \rho \frac{\partial \mathbf{u}}{\partial t} \quad (6)$$

with  $\rho$  being the material density. The force density  $\mathbf{f}_k$  can be expressed as consisting of  $\mathbf{f}_e$  in equation (3) and a yet to be determined component  $\mathbf{f}_m$

$$\mathbf{f}_k = -\mathbf{f}_e - \mathbf{f}_m \quad (7)$$

Finally, the third or material subsystem is

$$\nabla \cdot \mathbf{T}_m + \frac{\partial \mathbf{G}_m}{\partial t} = \mathbf{f}_m \quad (8)$$

The material stress tensor is represented in a generalized tensor expansion

$$\mathbf{T}_m = - \sum_{p,q \geq 0} \alpha^{pq} (\nabla \mathbf{u})^p \mathbf{H}^q - \mu_0 \mathbf{M} \mathbf{H} + \alpha^{10} : \nabla \mathbf{u} \quad (9)$$

with expansion coefficients  $\alpha^{pq}$ . The second term in (9) takes into account the magnetization state of the medium and the third term compensates for the independent magnetic field term in the summation. Since  $\mathbf{G}_m = \mathbf{0}$  it follows that equation (9), through the divergence operation, is directly related to the unknown force density  $\mathbf{f}_m$  in (7). Expanding (9) for the first three terms (subscripts 0 indicate a static bias field) yields

$$\mathbf{T}_m = -\alpha^{01} \cdot \mathbf{H} - \alpha^{02} : \mathbf{H}_0 \mathbf{H} - \mu_0 \mathbf{M}_0 \mathbf{H} \quad (10)$$

Furthermore, introducing the magnetization tensor  $\mathbf{e}$  such that

$$-\mathbf{e}^T = \alpha^{01} + \alpha^{02} \cdot \mathbf{H}_0 \quad (11)$$

with superscript  $\mathbf{T}$  denoting the transpose. After combining equations (11) and (10), one can take the divergence of equation (7) which results in

$$\mathbf{f}_k = \mu_0 \mathbf{J}_e \times \mathbf{H}_0 + \mu_0 \mathbf{M}_0 \cdot (\nabla \mathbf{H}) - \mathbf{e}^T : \nabla \mathbf{H} \quad (12)$$

The induced eddy current density  $\mathbf{J}_e$  in the specimen is found by solving a pulsed eddy current problem as presented in reference [2]. As can be seen the system consists of the well-known Lorentz forces (first term) and forces due to magnetization and magnetostriction (second and third terms respectively). Equation (12) forms the driving term in the elastic wave equation

$$(\lambda + \mu) \nabla \nabla \cdot \mathbf{u} + \mu \nabla^2 \mathbf{u} + \mathbf{f}_k = \rho \frac{\partial^2 \mathbf{u}}{\partial t^2} \quad (13)$$

where  $\lambda, \mu$  are the Lamé constants.

The boundary conditions between the field quantities outside (superscript 0) and inside (superscript i) the specimen can be specified as part of the continuity of stress

$$\mathbf{n} \cdot (\mathbf{T}_{\text{total}}^0 - \mathbf{T}_{\text{total}}^i) = \mathbf{0} \quad (14)$$

with the total stress tensor

$$\mathbf{T}_{\text{total}} = \frac{1}{2} \mu_0 (\mathbf{H} \cdot \mathbf{H}) \mathbf{I} - \mu_0 \mathbf{H} \mathbf{H} - \mathbf{e}^T \cdot \mathbf{H} - \mu_0 \mathbf{M} \mathbf{H} + \mathbf{c} : \nabla \mathbf{u} \quad (15)$$

Inserting equation (15) into (14) and assuming that the magnetization  $\mathbf{M}$  consists of a static field  $\mathbf{M}_0$  modified by a small bias field  $\mathbf{M}_S$  such that  $\mathbf{M} = \mathbf{M}_0 + \mathbf{M}_S$ , we obtain

$$\mathbf{n} \cdot (\mathbf{T}^0 - \mathbf{T}^i) = -\mu_0 (\mathbf{n} \cdot \mathbf{M}_S^i) (\mathbf{n} \cdot \mathbf{M}_0^i) \mathbf{n} \quad (16)$$

which reduces to zero if either the biased or static magnetization vector is tangential to the surface normal.

## SIMULATION RESULTS

As discussed in detail elsewhere [3,4], equation (13) is discretized by using the finite element method. The force density (12) is incorporated into equation (13) without magnetization and magnetostrictive forces such that

$$\mathbf{f}_k = \mu_0 \mathbf{J}_e \times \mathbf{H}_0 \quad (17)$$

where the induced eddy current density is computed based on a three cycle, 1 MHz centerfrequency, excitation current as shown in Figure 1.

Since the alignment of the transmitter coil is often of particular interest, two 8 wire-pair configurations of  $b = 3.2$  mm spacing and fixed as well as variable lift-off as shown in Fig. 2 are investigated in terms of their resulting radiation pattern. Under the assumption that  $\mu \mathbf{H}_0$  in equation (17) generates a uniform y-directed magnetic field of 1 Tesla, one obtains the simulated Lorentz force density as shown in Fig.3 for fixed and Fig.4 for variable wire lift-off.

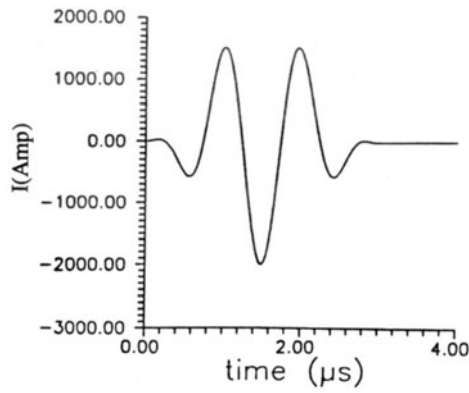


Fig. 1. Excitation current of 1MHz centerfrequency impressed in transmitter coil.

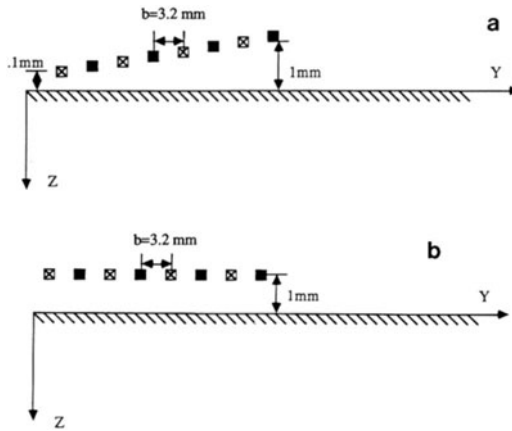


Fig. 2. Coil arrangement for 8 wire-pair EMAT transmitter. a) variable and b) fixed lift-off. Note, due to symmetry, only the right half plane is shown.

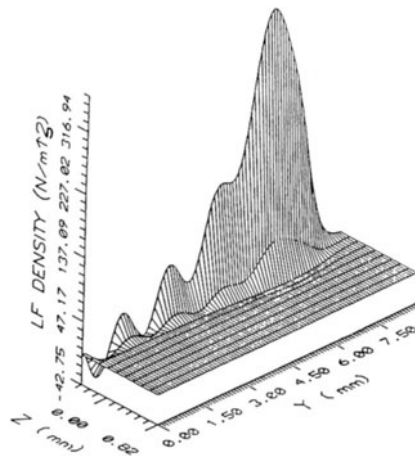


Fig. 3. Spatial Lorentz force distribution in specimen for fixed wire lift-off at time instance  $t= 3.2 \mu\text{s}$ .

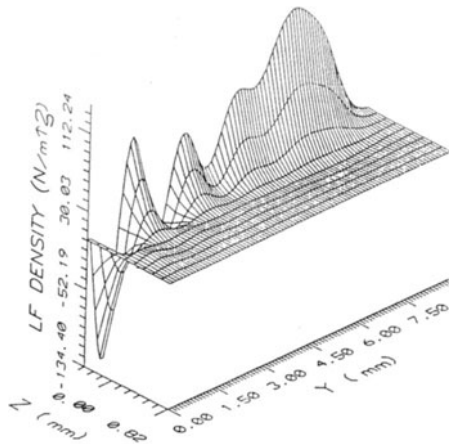


Fig. 4. Spatial Lorentz force distribution in specimen for variable wire lift-off at time instance  $t = 3.2 \mu\text{s}$ .

It is evident that the fixed lift-off configuration generates strong edge fields which influences the acoustic radiation pattern. For the radial particle displacement component (Figs. 5 and 6) the variable lift-off configuration produces separate surface pulses and a considerable acoustic wave leakage into the specimen. This observation is also evident in Figs. 7 and 8 where the time-amplitude (A-scan) response of the displacement field at locatios  $z = y = 21 \text{ mm}$  is considered.

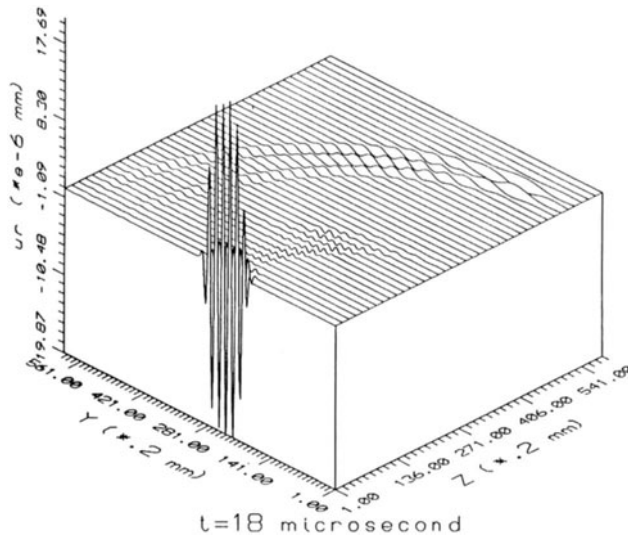


Fig. 5. Displacement field distribution at  $t=18\mu\text{s}$  and wire spacing of  $b = 3.2 \text{ mm}$  for variable wire lift-off.

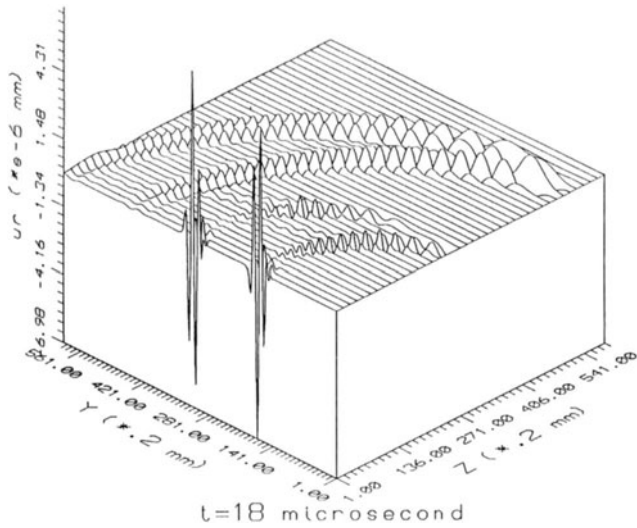


Fig. 6. Displacement field distribution at  $t=18\mu\text{s}$  and wire spacing of  $b = 3.2$  mm for fixed wire lift-off.

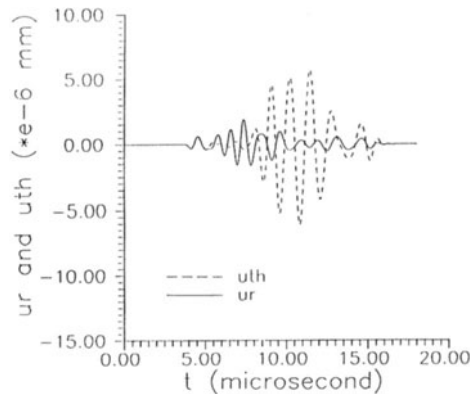


Fig. 7. Displacement response at spatial location  $z = y = 21$  mm due to variable wire lift-off.

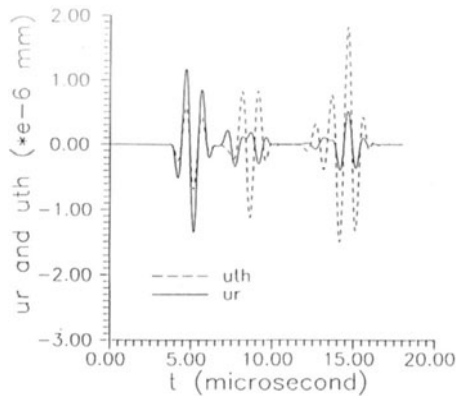


Fig. 8. Displacement response at spatial location  $z=y=21$  mm due to fixed wire lift-off.

## CONCLUSIONS

In this paper a unified conservation law description of the transient EMAT transduction process is developed. The separate accounting of electrical, mechanical and material subsystems permits the derivation of a complete set of governing equations and their associated boundary conditions. These underlying equations can be discretized and solved for the particle displacement field in two dimensions on a workstation type computer. Simulations of fixed versus variable wire lift-off transmitter coil configurations reveal significant changes in the acoustic wave propagation behavior in an isotropic elastic half-space due to the resulting nonuniform and uniform Lorentz force distributions.

## ACKNOWLEDGEMENT

This project is supported by the NDE and Sensor Technology Department, Timken Research, The Timken Company, Canton OH 44706.

## REFERENCES

1. W. J. Pardee and R. B. Thompson, "Half-Space Radiation by EMATs," *Journal of Nondestructive Testing*, Vol. 1, No. 3, pp. 157-181, 1980.
2. X.-W. Dai, R. Ludwig, and R. Palanisamy, "Numerical Simulation of Pulsed Eddy Current Nondestructive Testing Phenomena," *IEEE Trans. on Magnetics*, Vol. 26, No. 6, pp. 3089-3096, Nov. 1990.
3. R. Ludwig, X.-W. Dai, and R. Palanisamy, "Numerical Modeling of Electromagnetic Acoustic Transducer (EMAT) Phenomena," *Review of Progress in Quantitative NDE*, D.O. Thompson and D.E. Chimenti, eds., Vol. 10A, pp.845-852, Plenum Press, 1991.
4. R. Ludwig and X.-W. Dai, "Numerical Simulation of Electromagnetic Acoustic Transducer in the Time Domain," *J. Appl. Phy.*, Vol. 69, No. 1, pp. 89-98, 1991.